Electron - phonon scattering in noble metals containing dislocations

1996 J. Phys.: Condens. Matter 8 5891

(http://iopscience.iop.org/0953-8984/8/32/009)

J. Phys.: Condens. Matter **8** (1996) 5891–5904. Printed in the UK

Electron–phonon scattering in noble metals containing dislocations

F Sachslehner

Institut für Festkörperphysik der Universität Wien, Strudlhofgasse 4, A–1090 Wien, Austria

Received 27 November 1995, in final form 16 April 1996

Abstract. In the limit of small deformation (true strain $\varepsilon < 10\%$) it is possible to derive from curves of the deviation from Matthiessen's rule (DMR) for samples containing dislocations the anisotropy parameter of electron–phonon scattering (A_{ph}) as a function of temperature. In this case the fitted A_{ph}-curves for copper and silver samples based on the two-group model (TGM) are in excellent agreement with the theoretical calculation of Hasegawa and Kasuya. In contrast A_{ph}-curves derived from low-field Hall effect data within the (uncorrected) TGM are not directly suitable for DMR calculations due to the different averaging of relaxation times for the conductivity and the Hall effect. For understanding DMR curves with $10\% < \varepsilon < 100\%$ the two-group model is insufficient. Up to about 0.2 of normalized DMR seems to result from a DMR between small- and large-angle scattering.

1. Introduction

The importance of the anisotropy of electron–phonon scattering for electronic transport phenomena in noble metals has been known of for a long time [1]. Up to now it has seemed that the most reliable information about this topic has been derived from the low-field Hall effect (LFHE) measurements of Barnard [2, 3] by use of the two-group model (TGM) of the Fermi surface [1]. This was the basis on which the anisotropy parameters $A_{ph}(T)$ for electron–phonon scattering in ideally pure silver [2] and copper [3] were estimated.

However, these $A_{ph}(T)$-results extracted in the framework of the TGM from measurements of the LFHE did not seem to be very useful for the calculation of curves of the deviation of Matthiessen's rule (DMR) for copper samples containing dislocations [4]. As shown in an extensive analysis of the TGM [5] these $A_{ph}(T)$-values obtained from the LFHE (i) depend on the neck angle of the TGM and (ii) are expected to be influenced by the different averaging of relaxation times in the LFHE method compared with that in the conductivity or DMR method (which can be described by 'combined conductivities' [4]). Here it should be noted that in the case of the conductivity (or DMR) method the averaging of relaxation times is simpler than for the LFHE because no quadratic averaging and no averaging with the curvature of the Fermi surface is involved [5]. So it is not surprising that the extreme values of $A_{ph}(T)$ at low temperatures obtained from LFHE data by Barnard [3] are not the best choice for the description of the DMR curves for copper samples containing dislocations [4]; for samples with deformations $\varepsilon > 20\%$ even isotropic electron–phonon scattering seemed to be needed [4]. In this context the 'more isotropic' theoretical $A_{ph}(T)$-curve of Hasegawa and Kasuya [6] calculated for the ideal electrical resistivity of copper is of interest. This curve deviates considerably from Barnard's curve for copper [3] and will be checked for DMR calculations in the present paper.

0953-8984/96/325891+14$19.50

The TGM and the 'three-scatterer formula' turned out to be good concepts [4, 5, 7] for the description of the DMR step height of high-purity samples of the noble metals containing dislocations in the temperature range 4.2 K to 140 K. However, there remained always a considerable discrepancy between the experimental and modelled DMR curves in the temperature range from say 40 K to 100 K. The aim of the present paper is to investigate this discrepancy in more detail.

We calculate $A_{ph}(T)$-curves directly from experimental DMR curves with increasing dislocation densities assuming the validity of the three-scatterer DMR formula in order to see how these $A_{ph}(T)$-curves differ from published curves. For this purpose we take into account also the correct anisotropy parameters of electron–impurity scattering measured via the LFHE which vary considerably from material to material. So we hope to establish suitable $A_{ph}(T)$-curves for the experimental DMR curves of noble metals containing dislocations at least in the limit of low deformation.

In order to explain the discrepancy between the experimental and modelled DMR curves we consider a possible DMR contribution which cannot be explained by the TGM: the additional DMR which occurs if large-angle and small-angle scattering are present simultaneously and the relaxation time approximation fails [8]. This additional DMR contribution can be estimated approximately.

Finally important information for all three noble metals is obtained if different quantities such as the ideal electrical resistivity, the DMR, the intrinsic pure Hall constant and the $A_{ph}(T)$-curves are plotted on a temperature scale normalized to the Debye temperature.

2. Electron–phonon scattering in the TGM

It is well accepted [1, 2] that in the noble metals a significant anisotropy of electron–phonon scattering arises from the freezing out of Umklapp processes for belly electrons when the temperature is lowered. In the TGM this behaviour is simply described by a change in the anisotropy parameter A_{ph} for electron–phonon scattering:

$$A_{ph} = \tau_{NP}/\tau_{BP} \tag{1}$$

where τ_{NP} and τ_{BP} are the relaxation times on the Fermi surface for the neck and belly electrons of a pure sample (where the impurity contribution to the resistivity can be neglected), respectively. The most direct access to A_{ph} is from the low-field Hall coefficient R_H of a very pure sample material [5]:

$$-R_H = sf[1 + (r/s)A_{ph}^2 a]/(1 + A_{ph}b)^2. \tag{2}$$

a, b and f are integrals over the Fermi surface and depend on the choice of the neck angle of the TGM. a and b are independent of temperature. f depends only slightly on temperature via the lattice expansion but this can be neglected for the present investigation. r and s are correction parameters near unity which have to be taken into account if the LFHE and electrical resistivity data are based on unique relaxation times. This means that the temperature dependence of R_H is only given by the variation of A_{ph} with temperature. In the following we use only the physically indicated neck angles θ for the TGM as discussed in [5] and shown in table 1. This means in the cases of copper and gold that the corrected TGM is simplified by using the '$a = 0$ version'.

It follows from equation (2) that

$$A_{ph} = [-bR_H - \sqrt{f(-arR_H - b^2 sR_H - afrs)}]/(b^2 R_H + afr) \tag{3}$$

if $a = 0$, and thus

$$A_{\mathrm{ph}} = [-bR_{\mathrm{H}} - \sqrt{-fb^2sR_{\mathrm{H}}}]/(b^2R_{\mathrm{H}}) \tag{4}$$

or

$$s = [-R_{\mathrm{H}}(1 + A_{\mathrm{ph}}b)^2]/f. \tag{5}$$

Otherwise the ideal resistivity ρ_{P} can be written within the TGM as ($\hbar$ is Planck's constant)

$$1/\rho_{\mathrm{P}} = [e^2/(12\pi^3\hbar)](\tau_{\mathrm{BP}}c + \tau_{\mathrm{NP}}d) \qquad \text{with } c = \int_{\mathrm{B}} v\ \mathrm{d}S \qquad \text{and} \qquad d = \int_N v\ \mathrm{d}S. \tag{6}$$

Common terms in R_{H} (2) and ρ_{P} (6) are τ_{NP}, τ_{BP} and $b = d/c$. From combining equations (2) and (6) τ_{NP} and τ_{BP} could only be calculated correctly if the exact values of r and s were known. Here it should be noted that, especially for silver, the standard TGM ($r = s = 1$) does not work because R_{H} yields negative values for A_{ph} (see table 2).

Table 1. Parameters of the TGM used.

	Cu	Ag	Au
θ (deg)	18.7	16.5	17.9
a	0	0.061	0
b	0.219	0.150	0.214
f (10^{-11} m^3 C^{-1})	7.343	10.332	10.046
c (10^{27} m^{-1} s^{-1})†	2.156	2.317	2.004
d (10^{26} m^{-1} s^{-1})†	4.732	3.464	4.298

†Calculated by Watts [9].

In the case of the DMR for samples containing dislocations A_{ph} is involved via the three-scatterer formula [4]:

$$\delta(T, \varepsilon) = \sum_{j=1}^{3} \rho_j\rho_{j+1}bA_{j+2}(A_j - A_{j+1})^2\left(\sum_{j=1}^{3}\rho_j(1 + bA_j)^2A_{j+1}A_{j+2}\right)^{-1} \tag{7}$$

with the cyclic notation $\rho_4 = \rho_1$, $\rho_5 = \rho_2$, $A_4 = A_1$, $A_5 = A_2$, where A_j is the scattering anisotropy parameter of the jth scatterer (phonons, impurities and dislocations) and ρ_j is the resistivity of the jth scatterer on its own. The term b is the same as in (2).

3. Experimental details

3.1. Sample material

The sample material used for the present investigation was oxygen-annealed 99.99%-pure silver and gold described in [5], 99.9999%-pure copper from METALLEUROP (ME copper in the following) and oxygen-annealed 99.99%-pure copper from GOODFELLOW (GF copper in the following) described in [4, 7, 10]. The procedure for the DMR measurements and evaluation of experimental curves can be found in [4, 5, 7, 10].

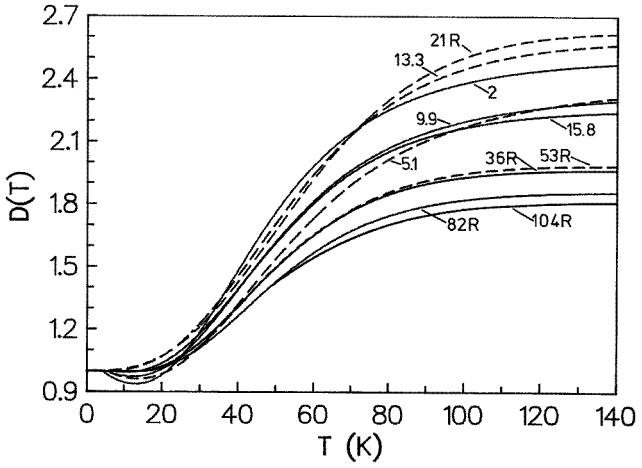

Figure 1. Normalized DMR curves for GF copper samples. The numbers indicate the true strain ε in %. R indicates deformation by rolling.

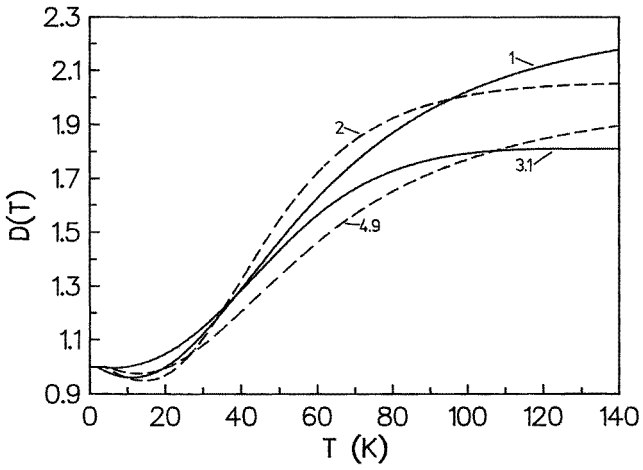

Figure 2. Normalized DMR curves for ME copper samples. Numbers: true strain ε in %.

3.2. DMR results used for the model calculations

Different aspects of DMR curves of the copper materials were published recently [4, 7, 10]. Usually the DMR is described as a function of temperature depending on the experimental dislocation resistivity $\rho_{d,ex}(T)$ or as the normalized quantity $D(T) = \rho_{d,ex}(T)/\rho_{d,ex}(4.2)$, where $\rho_{d,ex}(4.2)$ is the experimental dislocation resistivity at 4.2 K. Figure 1 shows a summary of smoothed experimental $D(T)$-curves for a set of GF copper samples ($\varepsilon = 2\%$ to 104%) to outline the principal behaviour of experimental DMR curves for noble metals. Similar curves are shown in figure 2 for some only slightly deformed ME copper samples. $D(T)$-curves for silver ($\varepsilon = 20\%$ to 116%) can be seen in figure 3. For a better overview the single data points are not shown, but the quality of data can be assessed elsewhere [4, 5, 10, 11] (see also figure 8). The curves of figures 1 to 3 as well as two curves for gold shown in [5] will be analysed in the following sections.

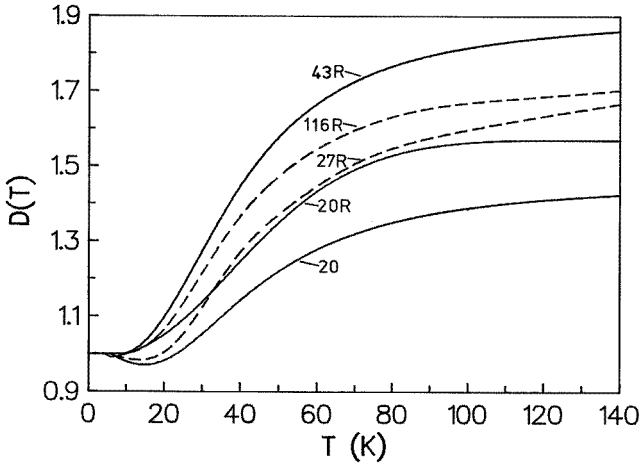

Figure 3. Normalized DMR curves for silver samples. Numbers: true strain ε in %. R indicates deformation by rolling.

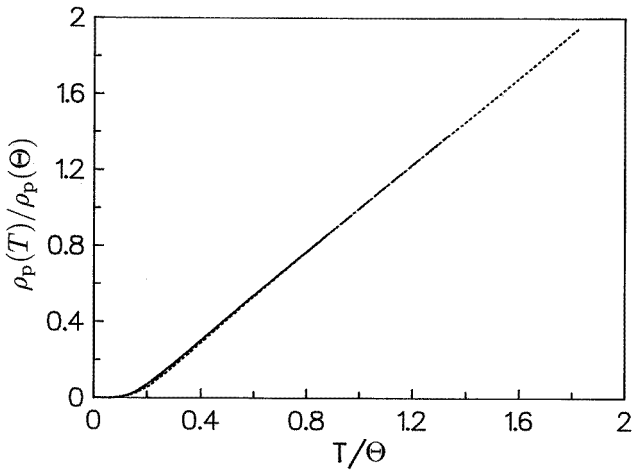

Figure 4. The ideal phonon resistivity ($\rho_P(T)$) of the noble metals normalized to the Debye temperature Θ. ——, copper; – – –, silver; and · · · · · ·, gold.

3.3. Debye normalization

It is well known [12] that a universal resistivity curve is obtained for many metals if the temperature is normalized to the Debye temperature Θ and the resistivity to its value at Θ. Figure 4 shows this picture for the ideal phonon resistivity of the noble metals [13] which is used in the following analysis. For Θ we use the values 346 K for copper, 226 K for silver and 164 K for gold [14]. Only the curve for gold in figure 4 has a small deviation, but the global behaviour of all three noble metals is the same.

Figure 5 shows the DMR curves at $\varepsilon \approx 100\%$ for the samples Cu100 (copper), Ag100 (silver) and Au100 (gold) of [5] normalized to Θ. Since $D(T)$ is only a weak function of temperature above 100 K the approximation $D(T)/D(130\ \mathrm{K}) \approx D(T)/D(\Theta)$ is used. For all three noble metals these reduced DMR curves lie within a certain band, which shows

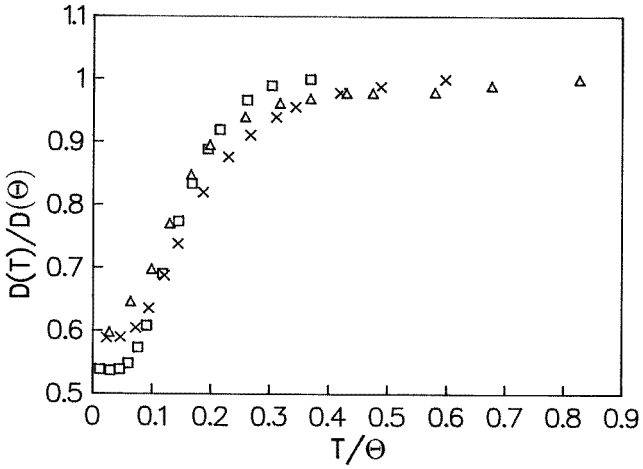

Figure 5. DMR curves of noble metals containing dislocations at $\varepsilon \approx 100\%$ (see the text) normalized to the Debye temperature Θ. □, copper; ×, silver; and △, gold.

that the DMR is also governed by very similar scattering behaviour in each noble metal. In contrast to the phonon resistivity in figure 4, the errors of the DMR curves are appreciably larger (error bars twice the symbol sizes have to be assumed). Moreover some genuine differences in the individual anisotropy parameters due to differences in the Fermi surface [5] should be monitored. The DMR curves at $\varepsilon \approx 50\%$ for the samples Cu50 (copper), Ag50 (silver) and Au50 (gold) of [5] give exactly the same band in a reduced plot, so the latter are not shown.

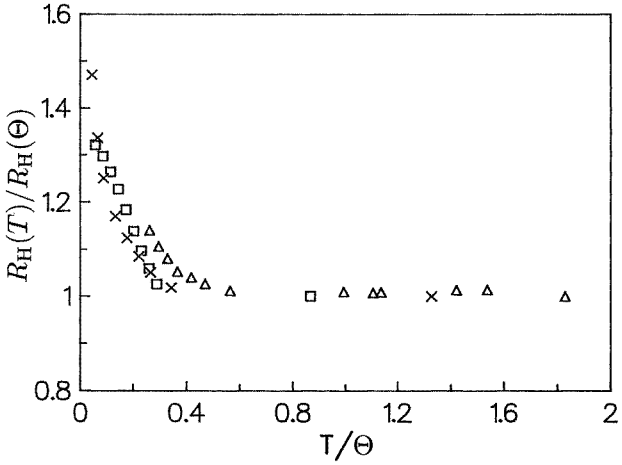

Figure 6. The low-field Hall coefficient of ideal pure noble metals (see the text) normalized to the Debye temperature Θ. □, copper; ×, silver; and (△) gold.

The low-field Hall coefficient of pure noble metals (electron–phonon scattering is dominant) normalized to Θ can be seen in figure 6 assuming $R_H(\Theta) \approx R_H(300)$. The $R_H(T)$-data are taken from the work of Barnard for ideally pure copper [3] and ideally pure silver [2]. The $R_H(T)$-data for gold are taken from tabulated results of Alderson *et al* [15]

as far as available in the low-field condition (only down to 40 K). Thus, only the influence of electron–phonon scattering and of different Fermi surfaces [5] is shown in figure 6. Obviously, the reduced R_H-data also lie within a certain band, like the DMR curves in figure 5. The data for copper and silver agree roughly, whereas for gold a tendency towards some deviation is indicated (the largest deviation from the spherical Fermi surface [5]). Unfortunately, up to now no LFHE data for pure gold have been available for temperatures between 40 K and 4.2 K.

From figures 4, 5 and 6 it may be concluded that the $A_{ph}(T)$-curves for all three noble metals reduced to the Debye temperature should also lie within some band. This means that if the $A_{ph}(T)$-function is known for at least for one metal, the $A_{ph}(T)$-curves for the other two metals could be estimated by applying the related Debye temperature.

4. Discussion

4.1. The anisotropy parameters of electron–phonon scattering

From a previous paper [5] it can be learnt that the DMR gives simpler and more reliable information about anisotropy parameters than the LFHE where the situation is complicated by the curvature of the Fermi surface and quadratic averaging effects (as long as the correction parameters are not known). This was shown particularly for A_{dis}, the anisotropy parameter for electron–dislocation scattering [5].

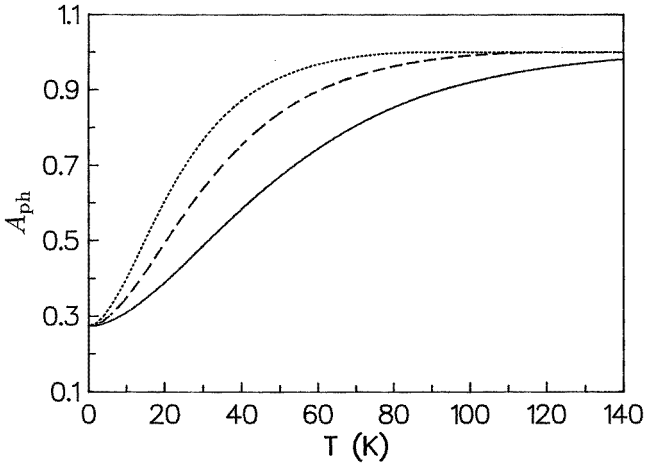

Figure 7. The anisotropy parameter of electron–phonon scattering (A_{ph}) for the noble metals as a function of temperature based on [6]. ——, copper (the A_{ph}–Cu-curve); - - - -, silver (the A_{ph}–Ag-curve); and · · · · · ·, gold (the A_{ph}–Au-curve).

For $A_{ph}(T)$ for copper it was shown very roughly in [4] that a quasi-isotropic $A_{ph}(T)$-curve (without being based on physical arguments) gives better fits to experimental DMR curves at low deformation ($\varepsilon < 20\%$) than the rather anisotropic curve of Barnard [3] derived from the LFHE for copper. This fact encourages us to use the nearly forgotten A_{ph}-curve of Hasegawa and Kasuya [6] calculated for copper (the HK-curve in the following) which lies in fact between the quasi-isotropic curve of [4] and Barnard's curve. The HK-curve was calculated by using a variational method and adjusted to the (ideal) measured electrical resistivity. This calculation was based on the band structures of Burdick and

the measured phonon spectrum. The HK-curve starts at 2 K with the value 0.27 (compare figure 7 described below), has the value 0.48 at 30 K, reaches the value 1.0 at 165 K and the value 1.04 at 300 K [6]. Although the investigations of Hasegawa and Kasuya [6, 16] have been cited many times [17–21], no attention has been paid to this curve, because it did not fit to the LFHE of copper [3] and had A_{ph}-values slightly larger than unity near room temperature. The latter problem was commented on in [6] as possibly resulting from a somewhat too large s–d hybridization effect in Burdick's band.

In order to have no contradiction to the successful assumption of isotropic electron–phonon scattering ($A_{ph} = 1$) near room temperature [5], we simply set the high-temperature part of the HK-curve to unity (which is a rather small correction to the maximum value 1.04 of the original curve) and smoothed the curve (using a curve-fitting program). The result can be seen in figure 7 as the full line (the A_{ph}–Cu-curve in the following). Additionally, as suggested above, we have reduced this curve by Θ(Cu) and multiplied the reduced values by Θ(Ag) and Θ(Au) in order to get also some estimate of the $A_{ph}(T)$-curves for silver and gold . These results are shown by the dashed (the A_{ph}–Ag-curve) and dotted lines (the A_{ph}–Au-curve) in figure 7.

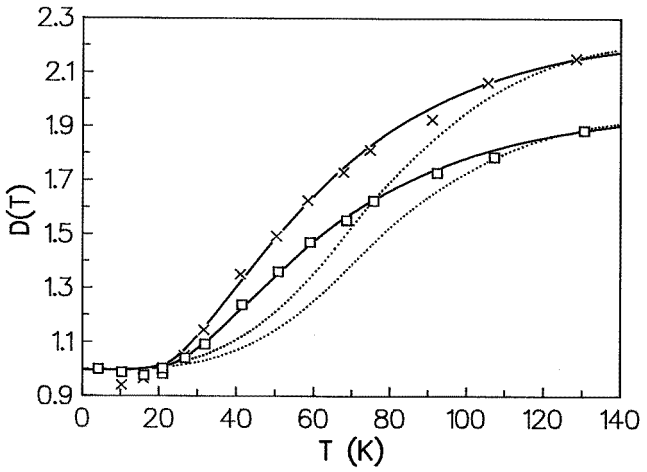

Figure 8. Fits of experimental DMR data of two ME copper samples (points: (×) $\varepsilon = 1\%$ and (□) $\varepsilon = 4.9\%$) using the A_{ph}–Cu-curve (——) and the A_{ph}-curve after Barnard [3] (· · · · · ·). The fitting condition is the coincidence of experimental data and models at 4.2 K and 130 K.

Figure 8 shows DMR fits (see equation (10) below) for ME copper samples with $\varepsilon = 1\%$ and $\varepsilon = 4.9\%$ using the A_{ph}–Cu-curve of figure 7. Excellent agreement with the experimental curves can be seen. The same good result is obtained for the GF copper samples with $\varepsilon = 5.1\%$ having a normalized DMR curve identical to that of the ME copper at 4.9%. Therefore the latter curve is not shown. For comparison the fits with the $A_{ph}(T)$-curve of Barnard obtained from the LFHE data are also shown in figure 8 (dotted lines); however, they deviate significantly from the fits with the A_{ph}–Cu-curve (after Hasegawa and Kasuya [6]) and the experimental points. Hence, we have the very clear result that also in case of electron–phonon scattering, the LFHE and electrical resistivity or DMR require different relaxation times if the different averaging of the two effects is not considered in the TGM (see the parameter s in (2) to (5)). For the case of A_{ph}-values at 300 K this was already indicated in [5].

Table 2 underlines the different $A_{ph}(T)$-values calculated from the LFHE data within the

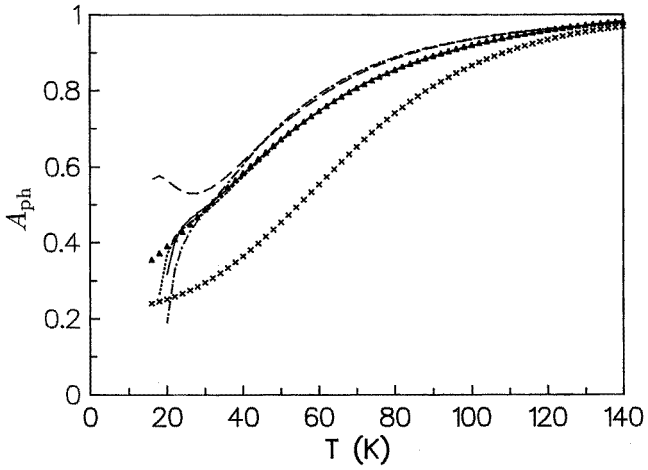

Figure 9. Fitted A_{ph}-curves for the experimental DMR curves of the ME copper shown in figure 2. ——, $\varepsilon = 4.9\%$; ·····, $\varepsilon = 1\%$; - - - -, $\varepsilon = 3.1\%$; — · —, $\varepsilon = 2\%$; ▲, the theoretical A_{ph}–Cu-curve and ×, the A_{ph}-curve for copper after Barnard [3] for comparison.

standard TGM ($r = s = 1$) using (3) related to the $A_{ph}(T)$-curves of figure 7. The same R_H-data as for figure 6 were used. The values of the second column of table 2 (Cu(LF)) are rather near to Barnard's $A_{ph}(T)$-curve [3] obtained from LFHE data. A graphical comparison of this Barnard curve with the A_{ph}–Cu-curve (figure 7) can be seen in figure 9.

Table 2. A comparison of $A_{ph}(T)$-values for the noble metals derived by two different methods. LF indicates evaluation from LFHE data, HK indicates values after the curves in figure 7 based on [6]. 'Neg' indicates negative values which are unphysical.

T (K)	Cu(LF)	Cu(HK)	Ag(LF)	Ag(HK)	Au(LF)	Au(HK)
10	—	0.309	Neg	0.348	—	0.399
20	0.214	0.389	Neg	0.492	—	0.603
30	0.257	0.486	Neg	0.637	—	0.767
40	0.321	0.583	0.079	0.754	0.496	0.871
50	0.935	0.671	0.208	0.838	0.647	0.932
60	0.485	0.745	0.334	0.896	0.747	0.968
70	0.585	0.806	—	0.936	0.808	0.988
80	0.681	0.853	0.466	0.962	0.842	0.998
90	0.773	0.891	—	0.980	0.860	1
100	0.860	0.919	—	0.991	—	1
110	—	0.942	—	0.998	—	1
120	—	0.958	—	1	—	1
130	—	0.971	—	1	—	1
300	0.949†	1	0.782†	1	0.927†	1

†Lattice expansion considered.

The largest discrepancy can be found for silver where—as shown in [5]—the largest averaging corrections (also for electron–phonon scattering) are expected. As shown in table 2 the use of the standard TGM with the physically indicated neck angle gives negative A_{ph}-values below 40 K in contrast to the values from the A_{ph}–Ag-curve of figure 7.

4.2. Calculation of anisotropy parameters from DMR curves

In [4] it was suggested that for the fits of experimental DMR curves (i) with $\varepsilon < 20\%$ quasi-isotropic $A_{ph}(T)$-curves but (ii) for $\varepsilon > 20\%$ isotropic $A_{ph}(T)$-curves would be a good choice. In order to see this behaviour in more detail we will determine $A_{ph}(T)$ explicitly from the normalized experimental DMR curves with A_{dis} and ρ_d fixed by a fit of the DMR step height ($D(130\ \mathrm{K}) - D(4.2\ \mathrm{K})$) where $A_{ph}(130\ \mathrm{K}) \approx 1$ is a well established value (to be precise, we use always for the step height fits $A_{ph}(130\ \mathrm{K}) = 0.97$ for copper and $A_{ph}(130\ \mathrm{K}) = 1$ for silver and gold according to figure 7). However, we have to be aware that for $T < 40$ K the relaxation time approximation is not expected to work very well, due to the influence of small-angle scattering [22].

Our experimental DMR curves have the form (see [5, 4])

$$\rho_{d,ex}(T) = \rho_d + \delta_{ipd} - \delta_{pi} \tag{8}$$

or the normalized form

$$D(T) = (\rho_d + \delta_{ipd} - \delta_{pi})/(\rho_d + \delta_{id}) \tag{9}$$

where $D(T) = \rho_{d,ex}(T)/\rho_{d,ex}(4.2)$ and $\rho_{d,ex}(T)$ is the experimental dislocation resistivity, being the difference in resistivity between a deformed sample and an undeformed reference sample [4]. ρ_d is the true dislocation resistivity. δ_{ipd} and δ_{pi} are DMRs originating in the deformed (three scatterers) and undeformed reference samples (two scatterers), respectively. δ_{id} equals the DMR δ_{ipd} at 4.2 K where the influence of the phonons can be neglected. For the DMR fits within the TGM it is assumed (as in [4, 5]) that the DMRs δ_{ipd} (δ_{id} at 4.2 K) and δ_{pi} in (9) can be described by equation (7) at least at the two fitting points at 4.2 K and 130 K (the fit of the DMR step height). The two free fitting parameters are A_{dis} and ρ_d which have to be adjusted in such a way that

$$\begin{aligned} &\text{(i) } \rho_d + \delta_{id} = \rho_{d,ex}(4.2\ \mathrm{K}) \\ &\text{(ii) } D(130\ \mathrm{K}) = [\rho_d + \delta(130\ \mathrm{K}, \varepsilon) - \delta(130\ \mathrm{K}, \varepsilon = 0)]/[\rho_d + \delta(4.2\ \mathrm{K}, \varepsilon)]. \end{aligned} \tag{10}$$

Since we use high-purity samples, we always find $\rho_{d,ex}(4.2\ \mathrm{K}) \approx \rho_d$, so the most important fitting parameter is A_{dis}. Making use of these resulting values, A_{dis} and ρ_d the full temperature dependence of $D(T)$ can be determined within the TGM if the curves of the ideal resistivity $\rho_P(T)$ [13] and $A_{ph}(T)$ (see figure 7) are used. The values of A_{im} and ρ_{im} of the various materials used in the following are given in table 3.

Table 3. Parameters of the TGM used.

	GF copper	ME copper	Ag	Au
ρ_{im} (nΩ cm)	0.598	1.182	2.3	2.3
A_{im}	0.26[a]	0.17[a]	0.32[b]	0.51[a]

[a] $s = 1$ with $a = 0$ was used (see (1) of [5]).
[b] $s = 1.17$ and $r = 1.50$ were used analogously to [5].

The first step of the determination of $A_{ph}(T)$ is to fit the experimental DMR curves (see section 3.2) at 4.2 K and 130 K according to (10) in order to obtain A_{dis} and ρ_d. As a second step we consider the full temperature variation of (10), already having good values for A_{dis} and ρ_d:

$$D(T) = [\rho_d + \delta(T, \varepsilon) - \delta(T, \varepsilon = 0)]/\rho_{d,ex}(4.2\ \mathrm{K}) \tag{11}$$

where we have replaced $\rho_d + \delta(4.2\ K, \varepsilon)$ in the second line of (10) by $\rho_{d,ex}(4.2\ K)$. We model the DMR $\delta(T, \varepsilon = 0)$ (approaching the DMR δ_{pi} of the reference sample (see (8)) as a fixed function of temperature by using a corresponding $A_{ph}(T)$-curve of figure 7. Then only the term $\delta(T, \varepsilon)$ (approaching the DMR δ_{ipd} of the deformed sample) contains some unknown variation of $A_{ph}(T)$ (see (7)). Hence, $A_{ph}(T)$ can be fitted or calculated explicitly (a quadratic equation in A_{ph}) from (11).

Figure 9 shows the fitted $A_{ph}(T)$-curves resulting from the experimental DMR curves for the ME copper (see figure 2). The 1% and 4.9% curves give A_{ph}-values agreeing perfectly with the (theoretical) A_{ph}–Cu-curve down to 20 K. The discrepancy from the Barnard curve (crosses) is obvious. Of course the experimental error of the $D(T)$-curves [4] which is larger at lower dislocation densities will be reflected by the fitted $A_{ph}(T)$-curves. Therefore not all curves with small ε are expected to agree equally with the A_{ph}–Cu-curve.

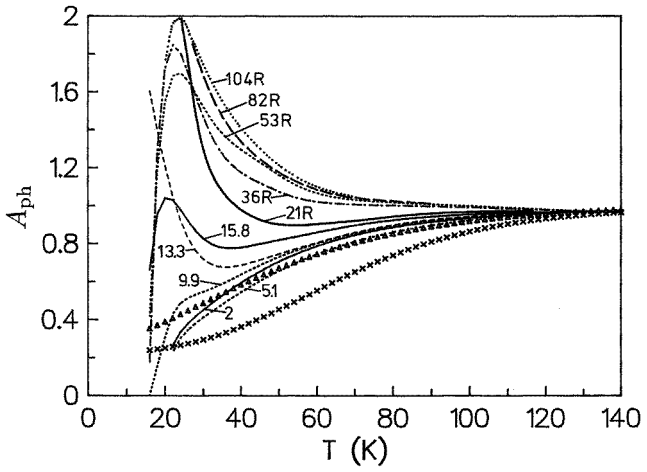

Figure 10. Fitted A_{ph}-curves for the experimental DMR curves of the GF copper shown in figure 1. The numbers indicate the true strain ε in %. R means deformation by rolling. △, the theoretical A_{ph}–Cu-curve and ×, the A_{ph}-curve for copper after Barnard [3] for comparison.

The fitted $A_{ph}(T)$-curves resulting from the $D(T)$-curves of the GF copper (see figure 1) are plotted in figure 10. Here only the 5.1% curve agrees perfectly with the A_{ph}–Cu-curve down to 40 K. In the temperature range where $T < 40$ K the curves from 2% to 15% are of similar character but deviate more at lower temperature. However, DMR curves for $\varepsilon > 20\%$ give not simple isotropic but anisotropic behaviour in the inverse direction with fitted values $A_{ph} > 1$ from 100 K down to nearly 20 K (a maximum is reached at around 20 K; figure 10). As there is no alternative explanation for such high A_{ph}-values, this increase of the fitted $A_{ph}(T)$-curves must be due to a DMR contribution which cannot be described by the formulae used up to now. As can be seen from (7) the only possibility for increasing the DMR in the model description is by increasing the differences in anisotropy parameters by using extremely high values of A_{ph}. We may conclude that the TGM is considerably in error if the dislocation density is increased or if other DMR contributions have to be taken into account. These points will be discussed in section 4.3.

Analogous $A_{ph}(T)$-curves fitted to the experimental $D(T)$-curves of silver and gold samples are shown in figure 11. The calculated curve for the silver sample with $\varepsilon = 20\%$ (deformed by tensile test) agrees rather well down to 30 K with the estimated A_{ph}–Ag-curve (see also figure 7). The $A_{ph}(T)$-curve for silver derived from the LFHE after Barnard [2] is

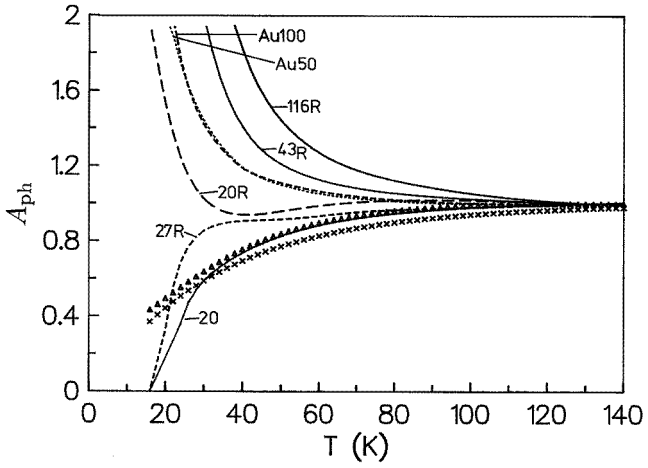

Figure 11. Fitted A_{ph}-curves for the experimental DMR of silver samples containing dislocations shown in figure 3 and the gold samples Au100 ($\varepsilon = 112\%$) and Au50 containing dislocations ($\varepsilon = 66\%$) of [5]. The numbers indicate ε for the silver samples (R means deformed by rolling). △, the 'theoretical' A_{ph}–Ag-curve and ×, the A_{ph}-curve for silver after Barnard [2] for comparison.

only somewhat lower. For the rolled silver and gold samples the same situation as for the rolled GF copper samples can be found. The fitted $A_{ph}(T)$-curves also reach a maximum near 20 K but at a value larger value than 2 (not shown). This means that the physics of DMRs for samples containing dislocations and of the electron–phonon scattering is very similar for all three noble metals. From the deviation of the fitted A_{ph}-values from the 'theoretical' A_{ph}–Cu-curve and A_{ph}–Ag-curve (see figures 10 and 11) it can be seen that the TGM becomes less reliable with increasing deformation and falling temperature.

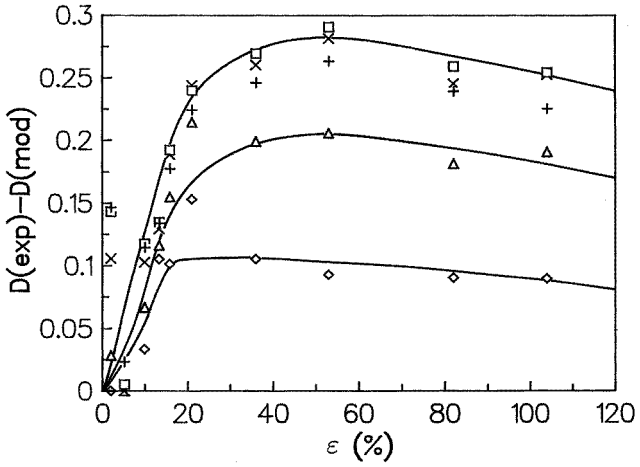

Figure 12. The difference between the experimental (D(exp)) and modelled (fitted) DMR curves (D(mod)) for the GF copper samples for some fixed temperatures: (◊) 30 K; (△) 40 K; (×) 50 K; (□) 60 K; and (+) 70 K. The full lines are guides for the eyes.

4.3. The discrepancy between experimental and modelled DMR curves

We confine the following analysis to the set of GF copper samples where the whole deformation range can be considered. For these samples the difference between experimental curves (D(exp)) and modelled (using the TGM) DMR curves (D(mod)) for some fixed temperatures can be seen in figure 12. The points for D(mod) were calculated choosing ρ_d and A_{dis} after the condition of (10) and using the A_{ph}–Cu-curve according to figure 7 (the usual fitting calculation for the DMR step height). The difference $D(\text{exp}) - D(\text{mod})$ increases with ε up to $\varepsilon \approx 20\%$ and then reaches an approximately constant level having the maximum value 0.28 (which means up to about 28% of the DMR step height $D(130\ \text{K}) - D(4.2\ \text{K})$) at 50 K to 60 K (compare figure 1). Two further details may be seen in figure 12. Firstly $D(\text{exp}) - D(\text{mod})$ is largest at 50 K to 60 K for all ε. Secondly there is a general tendency for a slight decrease of $D(\text{exp}) - D(\text{mod})$ with increasing ε after each maximum.

The discrepancy $D(\text{exp}) - D(\text{mod})$ found has to be interpreted as a DMR which is not included in the TGM. Here two points have to be considered. Firstly the TGM neglects the DMRs in the neck and belly groups of the conduction electrons [4] (apart from a possible interaction *between* neck and belly electrons). Secondly the TGM is based on the relaxation time approximation which, however, is expected to be violated in the case of small-angle scattering processes [22]. The fact that the maximum discrepancy occurs at around 50 K to 60 K could indicate a contribution to the DMR from small-angle scattering.

As discussed recently for copper [8] a contribution to the DMR arises even if isotropic small-angle scattering (SAS) and isotropic large-angle scattering (LAS) processes act together. Of course this contribution can be increased if different anisotropies are involved. Assuming that dislocation scattering is predominantly LAS [23], then this mechanism will produce a DMR from the combination of small-angle phonon scattering and dislocation scattering. Watts [9] has pointed out that calculating the DMR from this mechanism is complicated because, in effect, what is needed is the difference of two DMRs, one being from the SAS phonons combined with the dislocations plus LAS phonons, and the other from SAS phonons combined with the LAS phonons (even more complicated if impurities are also included). Rough preliminary calculations by Watts [9] based on his published curve [8] suggest a contribution to $D(T)$ of up to about 0.2 which should be largest in the temperature range where the SAS and LAS phonon scatterings are comparable. This corresponds to the temperature range where we have a discrepancy to explain. Unfortunately Watts does not expect the effect to disappear at low dislocation densities (D is normalized to the dislocation resistivity in the sample).

We suggest that the main part of the discrepancy $D(\text{exp}) - D(\text{mod})$ in figure 12 may be ascribed to combined DMR effects from SAS and LAS. The rest of the discrepancy could be thought to stem from contributions to the DMR *in* the neck and belly groups, which are neglected by the TGM [4]. Probably in the case of the low-deformation samples (where the TGM fits rather well), the smaller inaccuracy of the TGM is partially covered by the fitted parameters. So we may assume that the sources of the DMR discussed are sufficient for understanding the DMR for noble metals containing dislocations.

5. Conclusions

The temperature dependences of the DMR for samples containing dislocations and of the anisotropy of electron–phonon scattering are very similar for all three noble metals. This can be easily seen if a temperature scale normalized to the Debye temperature is used.

From the LFHE, in general a more extreme variation of anisotropic electron–phonon

scattering is derived compared to the DMR of samples containing dislocations that have low deformation. The reason for this is the different averaging of relaxation times for (i) the LFHE and electrical resistivity and (ii) the DMR.

If all of the parameters are considered carefully, especially the anisotropy parameters of electron–phonon scattering and electron–impurity scattering, the TGM is able to describe the temperature dependence of the DMR of samples containing dislocations rather well in the limit of small deformations ($\varepsilon < 10\%$). For samples with $\varepsilon \approx 20\%$ to 100% considerable deviations of the modelled DMR curves from the experimental curves occur in the temperature range 30 K to 60 K, contributing up to 28% of the normalized DMR step height.

The small-angle scattering processes seem to play an important role as regards the temperature dependence of the DMR of samples containing dislocations. The DMR which is missed in the calculations within the TGM can be ascribed mainly to a DMR contribution originating from large- and small-angle scattering.

Acknowledgments

The author thanks M Kočer for his contribution of doing the DMR experiments for the silver samples. The kind support by M Müller, B R Watts and V Gröger and their helpful discussions are gratefully acknowledged. The work was supported by the Fonds zur Förderung der wissenschaftlichen Forschung under Project 9930-PHY.

References

[1] Ziman J M 1960 *Electrons and Phonons* (Oxford: Clarendon)
[2] Barnard R D 1977 *J. Phys. F: Met. Phys.* **7** 673
[3] Barnard R D 1980 *J. Phys. F: Met. Phys.* **10** 2251
[4] Zürcher R, Müller M, Sachslehner F, Gröger V and Zehetbauer M 1995 *J. Phys.: Condens. Matter* **7** 3515
[5] Sachslehner F 1995 *J. Phys.: Condens. Matter* **7** 3913
[6] Hasegawa A and Kasuya T 1970 *J. Phys. Soc. Japan* **28** 75
[7] Sachslehner F 1994 *J. Phys.: Condens. Matter* **6** 11 229
[8] Watts B R 1994 *14th General Conf. of the Condensed Matter Division (Madrid)* Po.015 (see *Europhys. Conf. Abstracts* **18A** 326)
[9] Watts B R 1995 private communication
[10] Müller M 1994 *PhD Thesis* Universität Wien
[11] Kočer M 1996 *PhD Thesis* Universität Wien (in preparation)
[12] Dugdale J S 1977 *The Structures and Properties of Solids* vol 5, ed B R Coles (London: Edward Arnold) p 167
[13] Matula R A 1979 *J. Phys. Chem. Ref. Data* **8** 1147
[14] Schober H R and Dederichs P H 1981 *Landolt–Börnstein New Series* Group III, vol 13a, ed K-H Hellwege and J L Olsen (Berlin: Springer) p 10
[15] Alderson J E A, Farrell T and Hurd C M 1968 *Phys. Rev.* **174** 729
[16] Hasegawa A and Kasuya T 1968 *J. Phys. Soc. Japan* **25** 141
[17] Beaulac T P, Allen P B and Pinski F J 1982 *Phys. Rev.* B **26** 1549
[18] Beaulac T P, Pinski F J and Allen P B 1981 *Phys. Rev.* B **23** 3617
[19] Guénault A M and Lawson N S 1981 *J. Phys. F: Met. Phys.* **11** 2139
[20] Mann E and Schmidt H 1975 *Phys. Condens. Matter* **5** 33
[21] Guénault A M 1974 *J. Phys. F: Met. Phys.* **4** 256
[22] Watts B R 1996 to be published
[23] Watts B R 1989 *Dislocations in Solids* vol 8, ed F R N Nabarro (Amsterdam: Elsevier)